Resource

Cell Reports

Highly Efficient Genome Editing of Murine and Human Hematopoietic Progenitor Cells by CRISPR/Cas9

Graphical Abstract

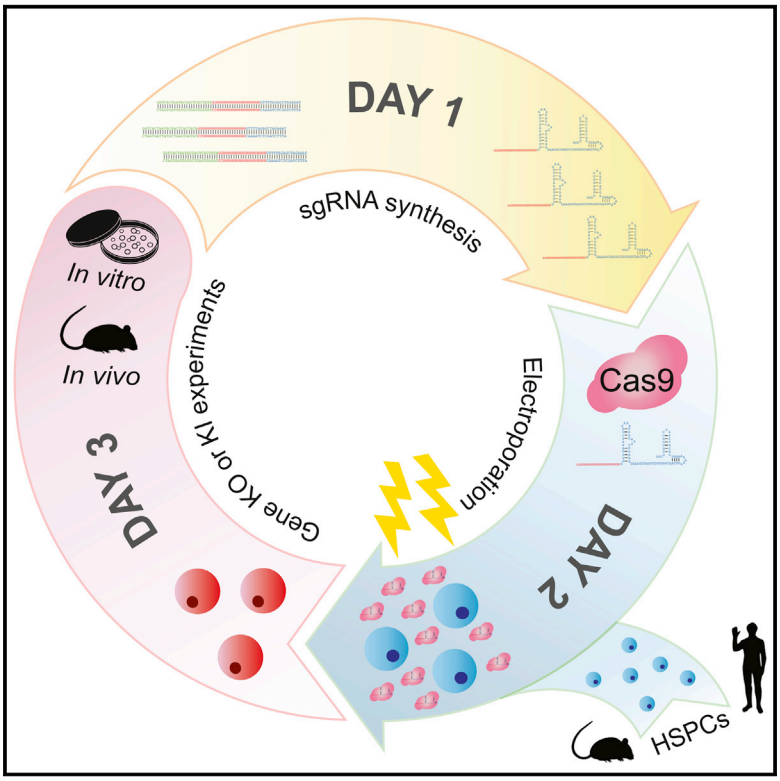

Authors

Michael C. Gundry, Lorenzo Brunetti, Angelique Lin, ..., Cliona M. Rooney, Margaret A. Goodell, Daisuke Nakada

Correspondence

goodell@bcm.edu (M.A.G.), nakada@bcm.edu (D.N.)

In Brief

Gundry et al. develop an efficient and simple method implementing CRISPR/Cas9-mediated gene disruption and HDR in murine and human HSPCs. This method enables quick evaluation of the function of genes by performing in vitro or transplantation assays using the modified HSPCs.

Highlights

- Gene knockout of primary murine HSPCs with efficiencies routinely higher than 60%
- Gene knockout of primary human HSPCs and T cells from 75% to 90%
- CRISPR/Cas9 homology-directed repair in >20% of primary human HSPCs

Gundry et al., 2016, Cell Reports *17*, 1453–1461
October 25, 2016
http://dx.doi.org/10.1016/j.celrep.2016.09.092

CellPress

Cell Reports
Resource

Highly Efficient Genome Editing of Murine and Human Hematopoietic Progenitor Cells by CRISPR/Cas9

Michael C. Gundry,[1,2,5,10] Lorenzo Brunetti,[2,5,7,10] Angelique Lin,[1,3,10] Allison E. Mayle,[1,2,5] Ayumi Kitano,[1] Dimitrios Wagner,[5,8,9] Joanne I. Hsu,[2,4,5] Kevin A. Hoegenauer,[1] Cliona M. Rooney,[5,6,8] Margaret A. Goodell,[1,2,5,6,8,*] and Daisuke Nakada[1,2,5,11,*]

[1]Department of Molecular and Human Genetics
[2]Stem Cells and Regenerative Medicine Center
[3]Integrative Molecular and Biomedical Sciences Program
[4]Translational Biology and Molecular Medicine Program
[5]Center for Cell and Gene Therapy
[6]Department of Pediatrics
Baylor College of Medicine, Houston, TX 77030, USA
[7]Centro di Ricerca Emato-Oncologica (CREO), University of Perugia, 06156 Perugia, Italy
[8]Texas Children's Hospital and Houston Methodist Hospital, Houston, TX 77030, USA
[9]Institute for Medical Immunology, Charité University Medicine Berlin, 13353 Berlin, Germany
[10]Co-first author
[11]Lead Contact
*Correspondence: goodell@bcm.edu (M.A.G.), nakada@bcm.edu (D.N.)
http://dx.doi.org/10.1016/j.celrep.2016.09.092

SUMMARY

Our understanding of the mechanisms that regulate hematopoietic stem/progenitor cells (HSPCs) has been advanced by the ability to genetically manipulate mice; however, germline modification is time consuming and expensive. Here, we describe fast, efficient, and cost-effective methods to directly modify the genomes of mouse and human HSPCs using the CRISPR/Cas9 system. Using plasmid and virus-free delivery of guide RNAs alone into Cas9-expressing HSPCs or Cas9-guide RNA ribonucleoprotein (RNP) complexes into wild-type cells, we have achieved extremely efficient gene disruption in primary HSPCs from mouse (>60%) and human (~75%). These techniques enabled rapid evaluation of the functional effects of gene loss of *Eed*, *Suz12*, and *DNMT3A*. We also achieved homology-directed repair in primary human HSPCs (>20%). These methods will significantly expand applications for CRISPR/Cas9 technologies for studying normal and malignant hematopoiesis.

INTRODUCTION

The ability to genetically manipulate the genomes of animal models or isolated cells has driven hematopoietic stem cell (HSC) research, revealing key mechanisms that control HSC self-renewal and differentiation. Numerous genetically engineered mouse models have contributed to our understanding of the pathways that control HSC maintenance and regeneration in physiological settings (Rossi et al., 2012). Although this approach produces invaluable insights and still remains a gold standard in studying HSC biology, large time and cost commitments are required to generate new mouse models, and the approach is generally not amenable to high-throughput studies. On the other hand, somatic engineering of hematopoietic stem/progenitor cell (HSPC) genomes has been achieved, in large, using retroviral vectors to either overexpress or knock down the expression of genes of interest (Rivière et al., 2012). This approach has been used to screen for both positive and negative regulators of HSC function from up to 100 candidate genes (Deneault et al., 2009; Hope et al., 2010). Although this approach allows investigators to quickly assess the function of multiple genes, retroviral transduction negatively impacts HSC function during in vitro culture, and retroviral genome integration is a serious concern when these engineered cells are used clinically (Hacein-Bey-Abina et al., 2003). A new method to edit the genomes of HSPCs should not only accelerate gene discovery research but also open up new clinical opportunities in using engineered HSPCs for gene therapy.

Among the several engineered nucleases enabling site-specific genome editing, the CRISPR-Cas9 system (Jinek et al., 2012) stands out since it does not require cumbersome engineering of nucleases for each target and only requires a 20-nt RNA sequence contained within a chimeric single-guide RNA (sgRNA) to drive the endonuclease Cas9 to its target sequence. Thus, CRISPR/Cas9 provides a versatile, modular, and cost-effective means to edit the genomes of multiple model systems (Hsu et al., 2014; Sternberg and Doudna, 2015). Several delivery methods have been used to perform CRISPR/Cas9-mediated gene editing of HSPCs, including lentiviral transduction (Heckl et al., 2014), plasmid DNA transfection (Mandal et al., 2014), or chemically modified RNA (Hendel et al., 2015), achieving up to

48% gene disruption in human HSPCs. While these studies have shown the enormous potential of HSPC gene editing by CRISPR/Cas9, a method that is highly efficient and simple, without the need for any cloning and nucleotide modifications, and that addresses clinical concerns of retroviral genome insertion is still lacking. We sought to develop simple strategies to perform CRISPR/Cas9-mediated gene editing in HSPCs with minimal manipulations and while avoiding viral integration into the HSPC genome. Here we describe fast, efficient, and cost-effective methods of CRISPR/Cas9-mediated gene editing in primary murine and human HSPCs, and we demonstrate that this method can be used to directly examine gene function.

RESULTS

Efficient Gene Disruption in Mouse HSPCs

We reasoned that transfecting HSPCs isolated from Cas9-expressing mice (Platt et al., 2014) with sgRNA would be an efficient method to edit the genome of HSPCs, since only the small RNA molecules would need to be introduced. To test this idea, we designed small guide RNAs to target the GFP gene (GFP-sg1) co-expressed in the Cas9-expressing mice. When we electroporated c-kit$^+$ HSPCs with in vitro-transcribed GFP-sg1, we observed highly efficient loss of GFP expression by flow cytometry, compared to cells electroporated with sgRNA against *Rosa26* (R26-sg) (Figure 1A). Although electroporation reduced the survival of HSPCs ~20% immediately after electroporation, cells maintained at least 80% viability throughout the experiment for up to 96 hr post-electroporation (Figure 1B). In this condition maintaining high viability, we found that 67% ± 4% of HSPCs lost GFP expression upon electroporation of GFP-sg1 (Figures S1A and S1B), demonstrating efficient gene editing with high cell viability. The frequency of GFP ablation exhibited a sgRNA dose-dependent increase, plateauing at 1 μg GFP-sg1 for 10^5 HSPCs per transfection (Figure 1C).

Because retroviral transduction is enhanced by culturing with cytokines to stimulate the cell cycle of quiescent HSPCs, we also tested whether brief in vitro exposure to cytokines in culture before sgRNA electroporation increased GFP gene editing. We electroporated Cas9-expressing HSPCs after varying the duration of culture. We found that a brief culture (1–3 hr) increased the frequency of GFP-negative cells from around 60% in fresh progenitors to a maximum of 85% ± 1% after 3 hr, without further increase after 12 hr (Figure 1D). In the context of this gene-editing strategy, incorporation of an optimized scaffold sequence previously shown to improve Cas9-mediated imaging (Chen et al., 2013) did not significantly increase the frequencies of gene disruption further (Figure S1C).

Because the c-kit$^+$ population contains various progenitors besides HSCs, we tested whether HSCs themselves undergo successful gene disruption upon transfection of sgRNAs. After electroporation of Cas9-expressing c-kit$^+$ cells with GFP-sg1, we sorted CD150$^+$CD48$^-$lineage$^-$Sca-1$^+$ cells (c-kit expression was attenuated within 1 hr of pre-culture before electroporation, Figure S1D) into semi-solid media, and we monitored colonies arising from these single HSCs for GFP ablation. Flow cytometry of individual colonies revealed that most HSC-derived colonies (40 of 48: 83%) lost GFP expression (representative three colonies shown in Figure 1E), whereas electroporation with or without sgRNA did not affect the clonality of HSCs compared to cultured, un-electroporated cells (Figure S1E). Thus, our method efficiently ablates genes in HSCs with minimum impact on HSC survival.

With the optimized sgRNA delivery method in hand, we next considered whether Cas9 protein pre-complexed with sgRNA to generate a ribonucleoprotein (RNP) particle (Kim et al., 2014; Lin et al., 2014; Schumann et al., 2015) also could be used to edit genes in murine HSPCs. Different amounts of GFP-sg1 were mixed with Cas9 protein, and the RNP complex was electroporated into HSPCs isolated from a mouse strain that ubiquitously expresses GFP (Schaefer et al., 2001). As shown in Figures 1F and 1G, ~70% of HSPCs lost GFP expression upon co-delivery of Cas9 protein and GFP-sg1. Two other sgRNAs against GFP also attenuated GFP expression in significant fractions of HSPCs (Figure S1G). Under this condition, HSPCs electroporated with Cas9 RNP maintained viability of >80% for up to 96 hr after electroporation (Figure S1F). Since loss of GFP expression is an indirect measure of genome editing, we directly examined insertion or deletion (indel) frequencies at the genomic level. First, we performed T7 endonuclease I (T7E1) assays and found that a significant fraction of HSPCs accrued indels (Figure 1H). We note that the T7E1 assay often underestimates the rate of indel formation, potentially due to self-hybridization of the alleles that carry the indel, incomplete duplex melting, and inefficient cleavage of single nucleotide indels (Schumann et al., 2015). To accurately determine the nature of the indels, we next performed high-throughput sequencing, which revealed that ~60% of HSPCs accrued small indels (Figure S1H; Table S2). These genomic analyses corroborated the flow cytometry data demonstrating that GFP alleles were mutated by the Cas9 RNP approach. Thus, this strategy allows us to study gene function directly in HSPCs in any genetic background.

Functional Assessment of Gene Disruption in Mouse HSPCs

We then tested whether targeted gene editing in HSPCs by CRISPR/Cas9 could be used to alter HSPC function. We chose to disrupt two polycomb-repressive complex 2 (PRC2) components *Eed* and *Suz12*, which are both found mutated in human leukemias (Shih et al., 2012). It has been shown that monoalleleic loss, but not biallelic loss, of *Eed* or *Suz12* confers proliferative advantages to HSPCs (Lee et al., 2015; Xie et al., 2014). We transfected wild-type HSPCs with Cas9-RNP complexes against *Rosa26*, *Eed*, or *Suz12*; plated them on semi-solid media; and serially replated the cells. Whereas most *Rosa26*-targeted HSPCs lost proliferative capacity upon the fourth replating, *Eed*- and *Suz12*-targeted HSPCs exhibited extensive proliferative capacity at the fourth passage (Figure 2A). T7E1 assays performed on HSPC cultures shortly (48 hr) after electroporation revealed that a substantial fraction of cells accrued indels in *Eed* and *Suz12* (Figure 2B). Sanger sequencing and tracking of indels by decomposition (TIDE) analysis (Brinkman et al., 2014) revealed that ~50% of the sequence reads accrued small indels between 4-bp deletion and 2-bp insertion (Figures S2A and S2B).

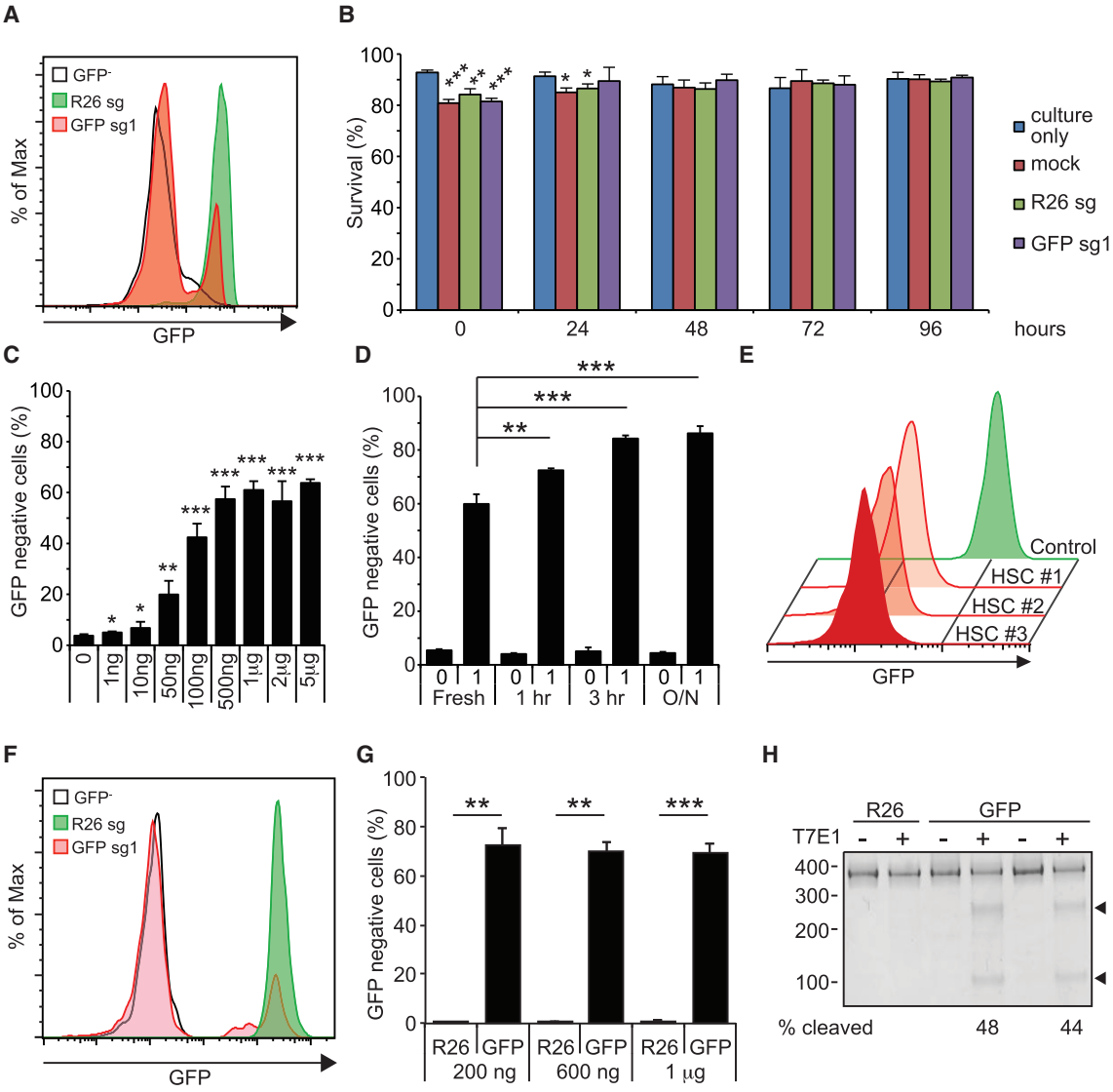

Figure 1. Gene Editing in Murine HSPCs

(A) A representative flow cytometry histogram showing efficient ablation of GFP by electroporating GFP-sg1 into Cas9-expressing HSPCs. Black histogram represents GFP$^-$ HSPCs, and green and red histograms represent *Rosa26* (R26)- and GFP-disrupted HSPCs, respectively (n = 3).

(B) Survival of HSPCs was determined by trypan blue staining of cells cultured without electroporation, cells mock electroporated without sgRNA, and cells electroporated with R26 or GFP sgRNA. 1 μg of sgRNA was used to electroporate 10^5 cells (n = 3).

(C) Deletion efficiencies of GFP exhibiting sgRNA dose-dependent response. A plateau in gene-editing efficiency was reached by 1 μg sgRNA/10^5 cells (n = 3).

(D) A brief culture of murine HSPCs for 1–3 hr increased gene-editing frequency, while overnight (O/N) culture did not further increase gene editing (n = 3).

(E) After electroporating c-kit$^+$ HSPCs with GFP-sg1, HSCs were sorted clonally into methylcellulose media. Most (40 of 48) HSC colonies exhibited loss of GFP expression, as shown by the representative flow cytometry histograms for three HSC-derived colonies from one donor mouse (n = 3 independent experiments).

(F) A representative histogram demonstrates efficient ablation of GFP expression by electroporating Cas9/GFP-sg1 RNP into GFP-expressing HSPCs (n = 3).

(G) Quantification of results in (F). Even as little as 200 ng GFP-sg1 efficiently ablated GFP upon delivery with Cas9 protein (1 μg).

(H) T7E1 assays performed with GFP amplicon derived from R26- or GFP-disrupted HSPCs. PCR amplicons were either treated (+) or untreated (–) with T7E1. Arrowheads indicate the bands with expected size assuming small indels, based on the Cas9 cleavage site. 1 μg of sgRNA was used to electroporate 10^5 Cas9-expressing cells unless otherwise noted. All data represent mean ± SD (*p < 0.05, **p < 0.01, and ***p < 0.001 by Student's t test). See also Figure S1.

We also cloned individual colonies at later passages and examined the editing status. T7E1 assay revealed that *Eed*- and *Suz12*-edited colonies acquired indels, and sequencing verified that they all acquired monoallelic loss of *Eed* or *Suz12* (Figures 2C–2F), consistent with the haploinsufficient function of *Eed* and Suz12 (Lee et al., 2015; Xie et al., 2014). These results establish that Cas9 RNPs can be used to perform gene editing in primary murine HSPCs regardless of genetic background, resulting in clear loss-of-function phenotypes.

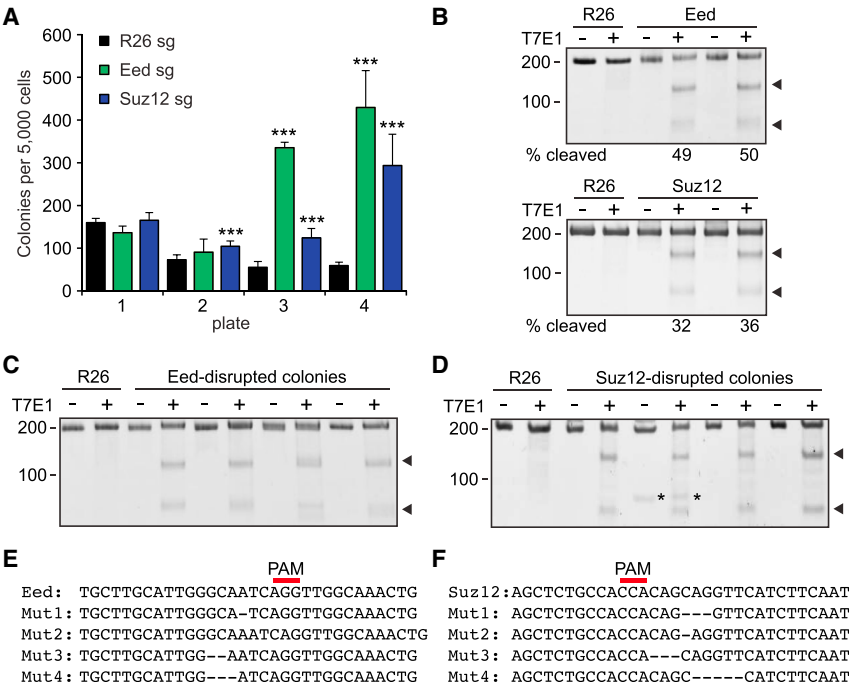

Figure 2. Editing Endogenous Genes in Murine HSPCs

(A) Gene editing of *Eed* or *Suz12* using Cas9-sgRNA RNP increased the ability of murine HSPCs to serially replate in culture; 1 μg Cas9 protein and 1 μg sgRNA were used (n = 4).

(B) T7E1 assays performed with *Eed* (top) or *Suz12* (bottom) amplicon derived from *Rosa26*- (R26), *Eed*-, or *Suz12*-disrupted HSPCs 48 hr after electroporation. The numbers below the gel image represent the cleavage efficiency determined by densitometric analysis (n = 3).

(C and D) T7E1 assays performed with *Eed* (C) or *Suz12* (D) amplicons derived from *Rosa26*- (R26), *Eed*-, or *Suz12*-disrupted colonies, with (+) or without (–) the nuclease (n = 4). Arrowheads indicate the bands with expected size based on the Cas9 cleavage site, whereas asterisks indicate nonspecific bands.

(E and F) Sequencing results of representative four clones each (of 12) after electroporating with Eed (E) or Suz12 (F) sgRNA. All colonies analyzed (Eed, 12/12; Suz12, 12/12) acquired indels. Red line represents the position of the protospacer adjacent motif (PAM) sequence. All data represent mean ± SD (***p < 0.001 by Student's t test). See also Figure S2.

Efficient Gene Disruption in Human HSPCs

Encouraged by the results obtained in mice, we assessed the feasibility and efficiency of our protocol in human hematopoietic cells. We first sought to target human CD45 (hCD45) in HL-60 cells, a human acute myeloid leukemia (AML) cell line. We electroporated HL-60 cells with Cas9/hCD45-sg RNPs testing three different CD45 guides. Strikingly, all three guides displayed very high efficiencies of disrupting CD45 expression (sg1, 98%; sg2, 91%; and sg3, 74%), as assessed by flow cytometry (Figure S3A). Two additional AML cell lines, OCI-AML2 and Kasumi, exhibited similar editing efficiencies (Figure 3A).

We also tested whether our protocol was capable of editing peripheral blood mononuclear cell (PBMC)-derived primary T lymphocytes. While resting T cells were resistant to CD45 editing (data not shown), activated T cells targeted with hCD45-sg1 exhibited efficient (86% ± 2%; n = 3) loss of CD45 (Figure 3A), with some residual $CD45^{bright}$ and $CD45^{mid}$ cells (Figure S3B). We performed high-throughput sequencing of unfractionated T cells as well as cells sorted based on CD45 expression ($CD45^{bright}$, $CD45^{mid}$, $CD45^{dim}$, and $CD45^{neg}$ cells), and we discovered that, while the unfractionated cells had an indel frequency of 83%, more than 95% of alleles in $CD45^{neg}$ and $CD45^{dim}$ cells and 40% of alleles in $CD45^{mid}$ cells had acquired indels (Figure S3B). Interestingly, $CD45^{dim}$ cells harbored 51% in-frame and 49% out-of-frame indels (Figure S3C), which may explain the residual CD45 expression (Figure S3C). Importantly, low indel frequencies (0.2%, 1.7%, and 0.4%; read depth: 924, 301, and 527) were observed at the top three predicted off-target (OT) sites (Figure 4B; Supplemental Experimental Procedures).

We then tested whether primary human $CD34^+$ HSPCs could be gene edited. To search for the optimal conditions, we first electroporated primary $CD34^+$ cells derived from umbilical cord blood with Cas9/hCD45-sg1 RNP using nine different electroporation parameters, and we performed flow cytometry 96 hr later to measure CD45 expression levels together with cell viability (Figure S3D). The optimized electroporation parameter (condition 9) was used for all further experiments. Since short-term ex vivo expansion is routinely exploited to increase transfection and transduction efficiency, we explored the impact of short cytokine exposure on transfection and gene disruption efficiency. We electroporated $CD34^+$ cells from single donors (n = 5) with mRNA encoding for GFP-fused Nucleophosmin 1 (GFP-NPM1) immediately after isolation, or after 24 or 48 hr of cytokine exposure, and we analyzed GFP expression 24 hr later. While fresh cells showed only 28% ± 13% GFP positivity, cells cultured for either 24 or 48 hr displayed transfection efficiencies higher than 75% (24 hr, 81% ± 12%; 48 hr, 78% ± 10%) (Figure S3E).

To assess whether CRISPR-mediated gene disruption efficiency was influenced by exposure to cytokines, we performed a similar experiment electroporating $CD34^+$ from single donors (n = 8) with Cas9/hCD45-sg1 RNP again at 0, 24, and 48 hr of culture, and we analyzed CD45 expression 4 days later. As expected, freshly isolated $CD34^+$ cells not exposed to cytokines exhibited limited loss of CD45 cell surface expression (8% ± 4%). However, gene disruption efficiency was significantly higher in cells cultured for 48 hr compared to 24 hr (73% ± 16% versus 41% ± 12%, p = 0.003) (Figure 3B), implying that the efficiency of gene disruption is dependent upon more than transfection efficiency. Importantly, CD34 expression remained unchanged even following efficient CD45 knockout (Figure 3C).

We also determined the impact of CRISPR-Cas9 delivery on human HSPC viability. $CD34^+$ cells from single donors were electroporated with Cas9 only or Cas9/hCD45-sg1 RNP or left

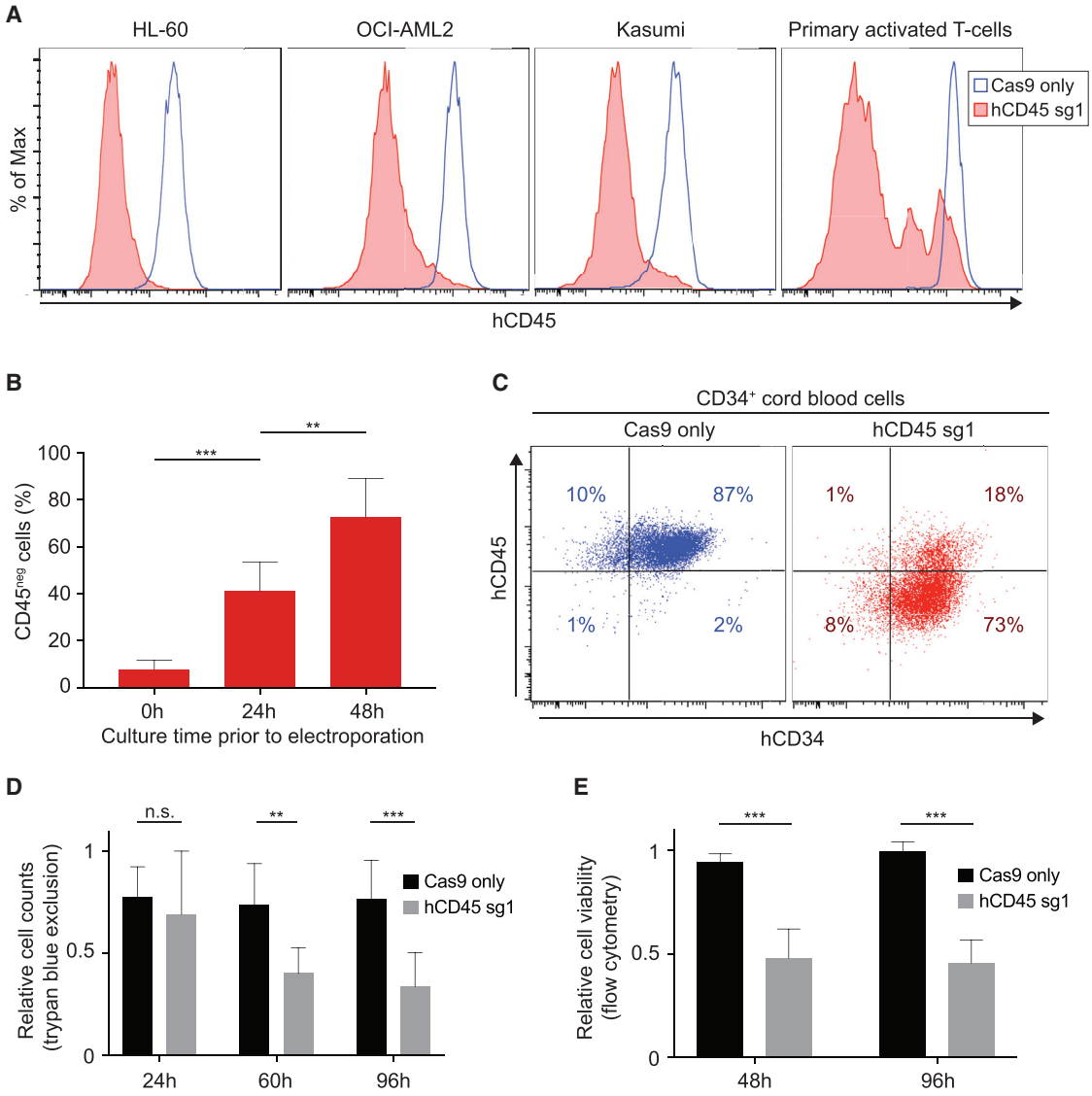

Figure 3. Efficient CD45 Knockout in Human Hematopoietic Cells

(A) Flow cytometry analysis of hCD45 expression in three AML cell lines and activated primary T cells 96 hr following electroporation with Cas9 only (blue) or Cas9/hCD45-sg1 RNP (red) is shown.

(B) Effects of pre-culture before electroporation on gene disruption efficiency. hCD45 loss was examined in $CD34^+$ cells cultured for 0, 24, and 48 hr in the presence of cytokines before electroporation with Cas9/hCD45-sg1 RNP. hCD45 expression was evaluated 4 days after electroporation. Each experiment (n = 8) was performed on $CD34^+$ cells isolated from single donors.

(C) Flow cytometry analysis of CD45 and CD34 expression in $CD34^+$ cells 96 hr following electroporation with Cas9 only (left) or Cas9/hCD45-sg1 RNP (right) is shown.

(D and E) Cell viability examined by trypan blue staining (D, n = 8) or flow cytometry (E, n = 6) of $CD34^+$ cells electroporated either with Cas9 only (black) or with Cas9/hCD45-sg1 RNP (gray) relative to non-electroporated cells at the indicated time points. The cell counts (D) or viability (E) of Cas9 only- and Cas9/hCD45-sg1-transfected cells was compared to the viable cell counts of non-electroporated cells.

All data represent mean ± SD; *p < 0.05, **p < 0.01, and ***p < 0.001 by non-parametric tests.

untreated in culture, and viable cell counts were recorded by trypan blue staining at 24, 60, and 96 hr after electroporation. Non-electroporated cells expanded in vitro, reaching 2.1 × 10^5 cells, 5 × 10^5 cells, and 1.1 × 10^6 cells at 24, 60, and 96 hr of culture, respectively, starting with 10^5 cells. Electroporated cells exhibited significant but acceptable cell loss in Cas9/hCD45-sg1 RNP-treated cells compared to non-electroporated cells (24 hr, 69% ± 31%; 60 hr, 40% ± 13%; 96 hr, 34% ± 17%; n = 8) (Figure 3D). Cell viability assessed by flow cytometry at 48 and 96 hr corroborated these results (48 hr, 48% ± 18%; 96 hr, 45% ± 11%; n = 6) (Figure 3E). These results are consistent with those reported by others using electroporation of

A

Target	sg1	sg2	Δ	Total
hCD45 (n=4)	75%	N/A	N/A	***75%***
hDNMT3A ex7 (n=5)	19%	5%	45%	***69%***
hDNMT3A ex10 (n=10)	11%	8%	67%	***86%***
hNR3C1 (n=5)	9%	9%	57%	***75%***

B

Target	T-cells (n=1)	CD34+ (n=3)
hCD45 OT1	0.2%	1.0%
hCD45 OT2	1.7%	7.0%
hCD45 OT3	0.4%	0.1%

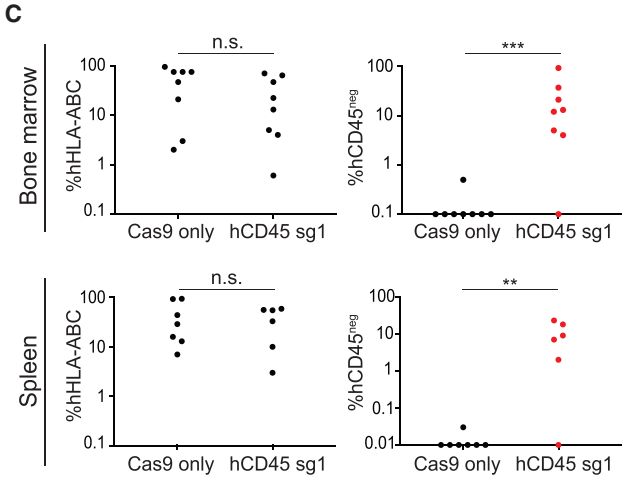

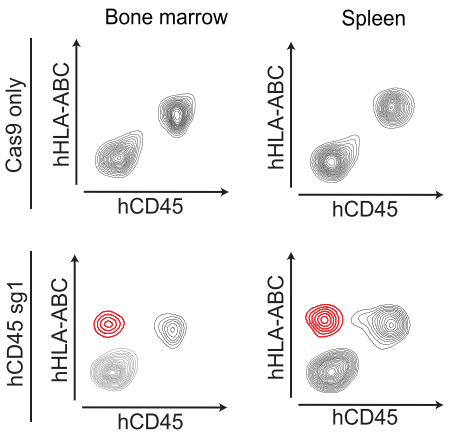

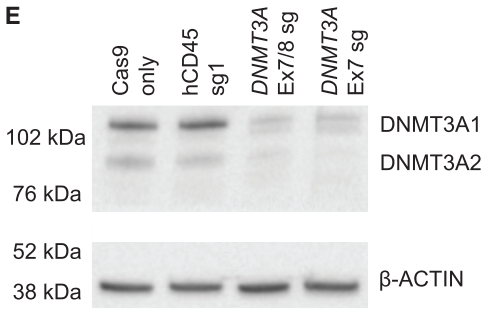

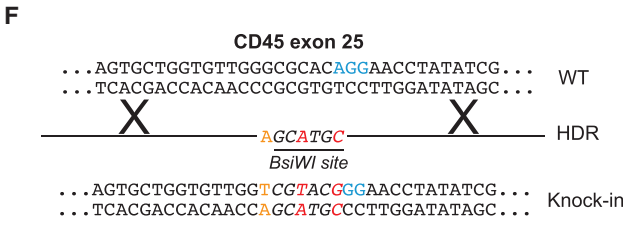

Allele	Read sequence	Allele frequency
WT	AGTGCTGGTGTTGGGCGCACAGGAACCTATATCG	47.9%
HDR	T T G	**24.2%**
HDR*	T G	**2.9%**
2bp del	--	1.6%
1bp del	-	1.6%
1bp ins	G	1.2%

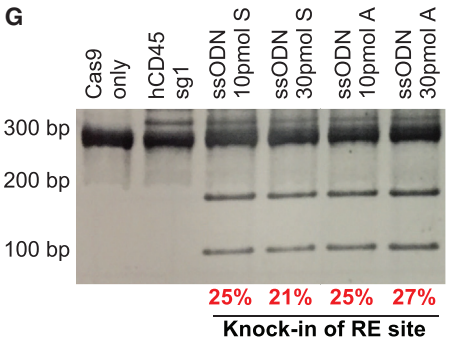

Figure 4. CRISPR-Cas9-Mediated Gene Disruption and HDR in Human HSPCs

(A) Indel frequencies at targeted loci. When multiple sgRNAs were used in the same experiment, sg1 indicates alleles with disruption of sg1 only, sg2 indicates alleles with disruption of sg2 only, and a triangle indicates alleles with a deletion between sg1 and sg2. Raw allele counts for each indel/deletion are found in Table S2.

(B) Indel frequencies at three predicted hCD45-sg1 OT sites. OT sites (OT1–3) were predicted using CRISPRscan (Moreno-Mateos et al., 2015).

(C) Plots showing percentages of human cells (left) in the bone marrow and the spleen of 16 NSG recipient mice (eight Cas9 only and eight Cas9/hCD45-sg1 RNP) and the fraction of engrafted human cells that have lost hCD45 (right) in Cas9 only (black) and Cas9/hCD45-sg1 RNP (red). Human CD34$^+$ cells from individual cord blood donors were electroporated with Cas9 only and Cas9/hCD45-sg1 RNP, and they were transplanted into sublethally irradiated NSG mice. Engraftment was analyzed 8 weeks post-transplant.

(legend continued on next page)

site-directed nucleases (De Ravin et al., 2016; Genovese et al., 2014).

CD45 knockout efficiency measured by flow cytometry (73% ± 16%) was confirmed by high-throughput sequencing of the hCD45 locus (75% ± 10%) (Figure 4A; Table S2). As in T cells, $CD34^+$ cells electroporated with Cas9/hCD45-sg1 (n = 3) displayed minimal OT cleavage (1.0%, 7.0%, and 0.1%; average read depth: 5,319, 5,164, and 5,089 at OT1, OT2, and OT3, respectively) (Figure 4B). To verify that the edited $CD34^+$ HSPCs maintained engraftment and multilineage differentiation capacity, we transplanted Cas9-only (n = 8) and Cas9/hCD45-sg1 RNP-edited cells (n = 8) into sub-lethally irradiated NOD scid gamma (NSG) mice. To avoid possible donor-dependent bias, each experimental pair (i.e., one Cas9-only replicate and one Cas9/hCD45-sg1 RNP-treated replicate) was performed on cells derived from a single cord blood. Bone marrow of 16/16 recipients and spleens of 13/16 recipients were successfully engrafted with human cells (Figure 4C). Importantly, we observed significant levels of engraftment by $hCD45^{neg}$ cells in the bone marrow of 7/8 mice and in the spleen of 5/8 mice transplanted with Cas9/hCD45-sg1 RNP-edited cells (Figures 4C, 4D, and S4A). Sequencing of the amplified human CD45 locus from bone marrow cells confirmed the presence of indels with frequencies consistent with flow cytometry data (Figure S4B). As expected for this time point (Goyama et al., 2015; McDermott et al., 2010), engrafted human HSPCs gave rise mainly to B and myeloid cells in the bone marrow in both Cas9 only- and Cas9/hCD45-sg1 RNP-engrafted mice, with no differences between these two groups (Figure S4C). The Cas9/hCD45-sg1 RNP-edited samples displayed no significant difference in CD45 gene disruption between B and myeloid cells (Figure S4D).

We also analyzed human $CD34^+$ HSPCs in one bone marrow sample in which 37% of engrafted human cells were CD45 negative. CD45 loss was evident in 40% of $CD34^+$ cells (Figure S4E) and 36% of the $CD34^+CD38^-$ population, which contained the most immature progenitor cells. These results establish that our method allows for efficient gene disruption of human $CD34^+$ HSPCs while retaining multilineage reconstitution capacity and the ability of these cells to engraft and expand in recipient mice. Given the known limitations of NSG mice to support robust generation of cells from all human hematopoietic lineages, such as T cells and erythroid cells, further assessment in additional models and longer time points will reveal whether the most long-term HSCs are successfully modified and viable after these treatments.

Multiple Guide Approach Allows for Rapid Deletion of Genes of Interest

To ensure functional ablation of a target gene and to facilitate rapid assessment of gene editing by PCR, larger deletions are often desirable. Thus, we synthesized guide RNA pairs targeting exons 7–14 of *DNMT3A*. We tested combinations of up to four guides per electroporation in HL-60 cells, assessing the frequency and spectra of deletions after 12 hr and the level of DNMT3A protein after 96 hr. All tested combinations of guides demonstrated efficient deletions and significantly diminished DNMT3A protein (Figure S4G).

We then targeted *DNMT3A* in primary $CD34^+$ cord blood cells. Guides targeting exons 7 and 8 were tested and the expected deletions were observed by PCR (Figure S4F). Importantly, the DNMT3A protein was nearly absent 96 hr after disruption of exon 7 or exons 7+8 (Figure 4E). To verify this result, *DNMT3A* exon 7 was targeted in $CD34^+$ cells enriched from an additional five cord blood samples, and high-throughput sequencing confirmed a gene disruption frequency of 69% ± 4% (Figure 4A; Table S2), suggesting that most cells likely experience loss of at least one allele, whereas many cells lose both alleles. To further validate the flexibility and efficiency of our approach, we targeted exon 10 of *DNMT3A* (n = 10) and exon 3 of *NR3C1* (n = 5) in $CD34^+$ cells, and high-throughput sequencing showed allelic disruption frequencies of 86% ± 14% and 75% ± 6%, respectively (Figures 4A and S4H; Table S2).

Efficient HDR-Mediated Gene Editing in Human HSPCs

Finally, we considered whether these editing strategies could be used to introduce specific point mutations into primary human HSPCs using Cas9-mediated homology-directed repair (HDR). HDR would enable specific lesions to be introduced in HSPCs, potentially correcting deleterious mutations or mimicking cancer-associated mutations. Single-stranded oligonucleotide HDR templates (ssODNs) were designed with symmetric or asymmetric homology arms (Richardson et al., 2016) to introduce three base pair changes, two of which resulted in the generation of a BsiWI site near the hCD45-sg1 spacer sequence (Figure 4F). After 48 hr of culture with cytokines, $CD34^+$ HSPCs were electroporated with the Cas9/hCD45-sg1 RNP along with either 10 or 30 pmol ssODNs. The addition of 10 or 30 pmol ssODNs did not significantly affect the viability (Figures S3F and S3G), although a trend toward lower viability after electroporation with a higher dose of ssODN was observed. Following BsiWI digestion of genomic DNA 24 hr after transfection, all samples with a donor template displayed a digested band, indicating

(D) Flow cytometry analysis of two engrafted NSG mice. Top panels show the engraftment of normal human cells ($CD45^{pos}$HLA-ABC^{pos}). Bottom panels show the presence of hCD45 knockout cells (highlighted in red) both in the bone marrow and the spleen.

(E) Western blot analysis of DNMT3A expression in $CD34^+$ cord blood cells 96 hr after electroporation with Cas9 only, Cas9/hCD45-sg1 RNP, Cas9/*DNMT3A* exon 7/8-sg (four sgRNAs) RNP, or Cas9/*DNMT3A* exon 7-sg (two sgRNAs) RNP is shown.

(F) Schematic representation of the CRISPR-mediated knockin (top). Three single-nucleotide changes, two of which (red) resulted in the formation of a *BsiWI* restriction site (italics), were introduced into hCD45 exon 25. The most commonly observed alleles from a representative sample (bottom), which included both precise (HDR; all three single-nucleotide changes) and imprecise (HDR*; two of three nucleotide changes) knockin events, were assessed by high-throughput sequencing, and their allele frequencies are displayed. The numbers in red represent frequencies of reads containing the *BsiWI* restriction site.

(G) A gel image of *BsiWI*-digested PCR amplicon prepared from $CD34^+$ cord blood cells targeted with Cas9/hCD45-sg1 (1 μg each) RNP and different single-stranded DNA oligonucleotides (ssODN) containing *BsiWI* sites. Both symmetric (S) and asymmetric (A) homology arms were tested. *BsiWI* digests the 282-bp amplicon with HDR editing into 172-bp and 110-bp fragments. The numbers below the gel represent efficiency of restriction site knockin (HDR+HDR*) as determined by high-throughput sequencing.

successful HDR (Figure 4G). High-throughput sequencing performed on these samples revealed efficient precise knockin (22%; range: 19%–25%) of the mutant allele (Figure 4F; Table S2). Additionally, many reads (1%–2%) displayed imprecise or partial knockin of the mutant allele (one of three or two of three bases) (Figure 4F; Table S2). Samples electroporated with only the donor template displayed no detectable mutant allele by high-throughput sequencing (data not shown). Thus, our method allows homology-directed gene editing at a substantial frequency in human HSPCs. Additional testing in multiple mouse and other animal models will be required to establish whether the most long-term HSCs are successfully edited.

DISCUSSION

The strategies we describe herein enable efficient gene editing, particularly loss-of-function studies, in both murine and human HSPCs directly. With the RNP-based methods, it is possible to generate gene-edited HSPCs within a week starting with conception of the study, including downtime for oligonucleotide synthesis. This is substantially shorter than editing HSPCs using lentiviral transduction, which requires cloning sgRNAs into lentiviral vectors, generation and quality control of lentiviral particles, and results in variable HSPC transduction efficiencies and risks of lentiviral integration in undesirable sites. Furthermore, electroporation of RNPs is a transient hit-and-run approach that obviates the need for a special mouse strain expressing Cas9, and it reduces concerns of constitutive Cas9 expression and OT cleavage. The costs of generating gene-edited HSPCs with these methods are substantially lower than those with lentiviral methods. Although commercially available Cas9 protein makes gene ablation with RNPs feasible, we also envision this strategy could be used for other Cas9 derivatives where transient effects may be desirable, such as CRISPR interference (Konermann et al., 2015; Qi et al., 2013).

One limitation of our protocol is that it lacks the ability to mark the cells that were successfully electroporated, unlike lentiviral transduction methods in which transduced cells can be marked by fluorescent proteins or by antibiotic resistance. However, with a gene-editing efficiency approaching 90% as we show for some targets, our method makes it possible to examine the molecular or phenotypic changes without selection for transfected cells. We have shown that deletion of *DNMT3A* from primary human $CD34^+$ cells leads to a precipitous reduction in DNMT3A protein levels in the population within 96 hr after electroporation.

We have observed that gene-editing efficiency is slightly more efficient in human than murine HSPCs. It is possible that this difference reflects developmental states, since the human cells are derived from cord blood rather than bone marrow. Additional optimization using murine HSPCs from the fetal liver or after mobilization may further increase the gene-editing efficiency.

Perhaps the most significant finding we observed was efficient HDR in human HSPCs. The ability to introduce specific mutations in HSPCs will enable the expanded study of cancer-driver mutations in AML and other hematologic diseases. More importantly, the repair of inherited mutations in both common and rare blood disorders using CRISPR may now be feasible without integration of viral vectors or delivery of plasmid DNA, representing a major stepping-stone toward therapeutic gene editing. We have not yet achieved detectable HDR frequencies in mouse HSPCs, and it is possible that a longer culture time prior to electroporation is necessary to activate this repair process in murine cells.

These remarkable knockout and HDR efficiencies in human HSPCs may suggest the possibility of broad and immediate utility. However, most ex vivo manipulations ultimately have been shown to impact function of the most long-term HSCs (Genovese et al., 2014; Hoban et al., 2015), and all of the available assays have limitations in their ability to assess bona fide HSC function. Therefore, caution in application of these strategies is still warranted.

In conclusion, we describe a fast, efficient, and cost-effective method to edit the genomes of both murine and human HSPCs based on the CRISPR/Cas9 system. The ability to quickly and efficiently edit primary HSPCs makes it possible to test the function of genetic variants identified in association with hematologic diseases, such as leukemia or bone marrow failure. Moreover, the high efficiency offers the possibility to perform large-scale combinatorial gene editing in HSPCs to model complex mutational landscapes.

EXPERIMENTAL PROCEDURES

Production of sgRNA and Electroporation

Protospacer sequences for each target gene were identified using the CRISPRscan algorithm (http://www.crisprscan.org) (Moreno-Mateos et al., 2015). DNA templates for sgRNAs were made using the protocol described by Li et al. (2013) using primers listed in Table S1. The sgRNA (1 μg) was electroporated into 1 × 10^5 Cas9-expressing c-kit^+ murine HSPCs after 1–3 hr of culture. The optimized electroporation condition for murine HSPCs was 1,700 V, 20 ms, and one pulse, using a Neon transfection system (Thermo Fisher Scientific). To electroporate Cas9-sgRNA RNPs, 200 ng to 1 μg sgRNA was incubated with 1 μg Cas9 protein (PNA Bio) for 10–15 min at room temperature and electroporated as above. Human $CD34^+$ cells were isolated by AutoMACS (Miltenyi Biotec) using CD34 microbeads, and they were electroporated as described for murine cells except the optimized electroporation condition was 1,600 V, 10 ms, and three pulses. See the Supplemental Experimental Procedures for details.

Statistical Analysis

For comparisons involving two groups, unpaired Student's t tests (two-tailed) or non-parametric tests were used. See the figure legends for details.

ACCESSION NUMBERS

The accession number for the data reported in this paper is NCBI Sequence Read Archive: PRJNA339433.

SUPPLEMENTAL INFORMATION

Supplemental Information includes Supplemental Experimental Procedures, four figures, and two tables and can be found with this article online at http://dx.doi.org/10.1016/j.celrep.2016.09.092.

AUTHOR CONTRIBUTIONS

M.C.G., L.B., A.L., A.E.M., M.A.G., and D.N. designed and discussed experiments. M.C.G., L.B., A.L., A.E.M., A.K., D.W., and J.I.H. performed experiments. M.C.G., L.B., and K.A.H. analyzed the sequencing data. C.M.R. provided reagents. All authors analyzed data. M.C.G., L.B., A.L., M.A.G., and D.N. wrote and edited the paper with input from all authors.

ACKNOWLEDGMENTS

This work was supported by the Cancer Prevention and Research Institute of Texas (RP16028, RP140001, and R1201), the Gabrielle's Angel Foundation for Cancer Research, the Evans Foundation, and the NIH (DK092883, CA183252, CA125123, P50CA126752, CA193235, and DK107413). M.C.G. is supported by Baylor Research Advocates for Student Scientists. Flow cytometry was partially supported by the NIH (National Center for Research Resources grant S10RR024574, National Institute of Allergy and Infectious Diseases AI036211, and National Cancer Institute P30CA125123) for the Baylor College of Medicine Cytometry and Cell Sorting Core.

Received: March 28, 2016
Revised: July 1, 2016
Accepted: September 28, 2016
Published: October 25, 2016

REFERENCES

Brinkman, E.K., Chen, T., Amendola, M., and van Steensel, B. (2014). Easy quantitative assessment of genome editing by sequence trace decomposition. Nucleic Acids Res. *42*, e168.

Chen, B., Gilbert, L.A., Cimini, B.A., Schnitzbauer, J., Zhang, W., Li, G.W., Park, J., Blackburn, E.H., Weissman, J.S., Qi, L.S., and Huang, B. (2013). Dynamic imaging of genomic loci in living human cells by an optimized CRISPR/Cas system. Cell *155*, 1479–1491.

De Ravin, S.S., Reik, A., Liu, P.Q., Li, L., Wu, X., Su, L., Raley, C., Theobald, N., Choi, U., Song, A.H., et al. (2016). Targeted gene addition in human CD34(+) hematopoietic cells for correction of X-linked chronic granulomatous disease. Nat. Biotechnol. *34*, 424–429.

Deneault, E., Cellot, S., Faubert, A., Laverdure, J.P., Fréchette, M., Chagraoui, J., Mayotte, N., Sauvageau, M., Ting, S.B., and Sauvageau, G. (2009). A functional screen to identify novel effectors of hematopoietic stem cell activity. Cell *137*, 369–379.

Genovese, P., Schiroli, G., Escobar, G., Di Tomaso, T., Firrito, C., Calabria, A., Moi, D., Mazzieri, R., Bonini, C., Holmes, M.C., et al. (2014). Targeted genome editing in human repopulating haematopoietic stem cells. Nature *510*, 235–240.

Goyama, S., Wunderlich, M., and Mulloy, J.C. (2015). Xenograft models for normal and malignant stem cells. Blood *125*, 2630–2640.

Hacein-Bey-Abina, S., Von Kalle, C., Schmidt, M., McCormack, M.P., Wulffraat, N., Leboulch, P., Lim, A., Osborne, C.S., Pawliuk, R., Morillon, E., et al. (2003). LMO2-associated clonal T cell proliferation in two patients after gene therapy for SCID-X1. Science *302*, 415–419.

Heckl, D., Kowalczyk, M.S., Yudovich, D., Belizaire, R., Puram, R.V., McConkey, M.E., Thielke, A., Aster, J.C., Regev, A., and Ebert, B.L. (2014). Generation of mouse models of myeloid malignancy with combinatorial genetic lesions using CRISPR-Cas9 genome editing. Nat. Biotechnol. *32*, 941–946.

Hendel, A., Bak, R.O., Clark, J.T., Kennedy, A.B., Ryan, D.E., Roy, S., Steinfeld, I., Lunstad, B.D., Kaiser, R.J., Wilkens, A.B., et al. (2015). Chemically modified guide RNAs enhance CRISPR-Cas genome editing in human primary cells. Nat. Biotechnol. *33*, 985–989.

Hoban, M.D., Cost, G.J., Mendel, M.C., Romero, Z., Kaufman, M.L., Joglekar, A.V., Ho, M., Lumaquin, D., Gray, D., Lill, G.R., et al. (2015). Correction of the sickle cell disease mutation in human hematopoietic stem/progenitor cells. Blood *125*, 2597–2604.

Hope, K.J., Cellot, S., Ting, S.B., MacRae, T., Mayotte, N., Iscove, N.N., and Sauvageau, G. (2010). An RNAi screen identifies Msi2 and Prox1 as having opposite roles in the regulation of hematopoietic stem cell activity. Cell Stem Cell *7*, 101–113.

Hsu, P.D., Lander, E.S., and Zhang, F. (2014). Development and applications of CRISPR-Cas9 for genome engineering. Cell *157*, 1262–1278.

Jinek, M., Chylinski, K., Fonfara, I., Hauer, M., Doudna, J.A., and Charpentier, E. (2012). A programmable dual-RNA-guided DNA endonuclease in adaptive bacterial immunity. Science *337*, 816–821.

Kim, S., Kim, D., Cho, S.W., Kim, J., and Kim, J.S. (2014). Highly efficient RNA-guided genome editing in human cells via delivery of purified Cas9 ribonucleoproteins. Genome Res. *24*, 1012–1019.

Konermann, S., Brigham, M.D., Trevino, A.E., Joung, J., Abudayyeh, O.O., Barcena, C., Hsu, P.D., Habib, N., Gootenberg, J.S., Nishimasu, H., et al. (2015). Genome-scale transcriptional activation by an engineered CRISPR-Cas9 complex. Nature *517*, 583–588.

Lee, S.C., Miller, S., Hyland, C., Kauppi, M., Lebois, M., Di Rago, L., Metcalf, D., Kinkel, S.A., Josefsson, E.C., Blewitt, M.E., et al. (2015). Polycomb repressive complex 2 component Suz12 is required for hematopoietic stem cell function and lymphopoiesis. Blood *126*, 167–175.

Li, D., Qiu, Z., Shao, Y., Chen, Y., Guan, Y., Liu, M., Li, Y., Gao, N., Wang, L., Lu, X., et al. (2013). Heritable gene targeting in the mouse and rat using a CRISPR-Cas system. Nat. Biotechnol. *31*, 681–683.

Lin, S., Staahl, B.T., Alla, R.K., and Doudna, J.A. (2014). Enhanced homology-directed human genome engineering by controlled timing of CRISPR/Cas9 delivery. eLife *3*, e04766.

Mandal, P.K., Ferreira, L.M., Collins, R., Meissner, T.B., Boutwell, C.L., Friesen, M., Vrbanac, V., Garrison, B.S., Stortchevoi, A., Bryder, D., et al. (2014). Efficient ablation of genes in human hematopoietic stem and effector cells using CRISPR/Cas9. Cell Stem Cell *15*, 643–652.

McDermott, S.P., Eppert, K., Lechman, E.R., Doedens, M., and Dick, J.E. (2010). Comparison of human cord blood engraftment between immunocompromised mouse strains. Blood *116*, 193–200.

Moreno-Mateos, M.A., Vejnar, C.E., Beaudoin, J.D., Fernandez, J.P., Mis, E.K., Khokha, M.K., and Giraldez, A.J. (2015). CRISPRscan: designing highly efficient sgRNAs for CRISPR-Cas9 targeting in vivo. Nat. Methods *12*, 982–988.

Platt, R.J., Chen, S., Zhou, Y., Yim, M.J., Swiech, L., Kempton, H.R., Dahlman, J.E., Parnas, O., Eisenhaure, T.M., Jovanovic, M., et al. (2014). CRISPR-Cas9 knockin mice for genome editing and cancer modeling. Cell *159*, 440–455.

Qi, L.S., Larson, M.H., Gilbert, L.A., Doudna, J.A., Weissman, J.S., Arkin, A.P., and Lim, W.A. (2013). Repurposing CRISPR as an RNA-guided platform for sequence-specific control of gene expression. Cell *152*, 1173–1183.

Richardson, C.D., Ray, G.J., DeWitt, M.A., Curie, G.L., and Corn, J.E. (2016). Enhancing homology-directed genome editing by catalytically active and inactive CRISPR-Cas9 using asymmetric donor DNA. Nat. Biotechnol. *34*, 339–344.

Rivière, I., Dunbar, C.E., and Sadelain, M. (2012). Hematopoietic stem cell engineering at a crossroads. Blood *119*, 1107–1116.

Rossi, L., Lin, K.K., Boles, N.C., Yang, L., King, K.Y., Jeong, M., Mayle, A., and Goodell, M.A. (2012). Less is more: unveiling the functional core of hematopoietic stem cells through knockout mice. Cell Stem Cell *11*, 302–317.

Schaefer, B.C., Schaefer, M.L., Kappler, J.W., Marrack, P., and Kedl, R.M. (2001). Observation of antigen-dependent CD8+ T-cell/ dendritic cell interactions in vivo. Cell. Immunol. *214*, 110–122.

Schumann, K., Lin, S., Boyer, E., Simeonov, D.R., Subramaniam, M., Gate, R.E., Haliburton, G.E., Ye, C.J., Bluestone, J.A., Doudna, J.A., and Marson, A. (2015). Generation of knock-in primary human T cells using Cas9 ribonucleoproteins. Proc. Natl. Acad. Sci. USA *112*, 10437–10442.

Shih, A.H., Abdel-Wahab, O., Patel, J.P., and Levine, R.L. (2012). The role of mutations in epigenetic regulators in myeloid malignancies. Nat. Rev. Cancer *12*, 599–612.

Sternberg, S.H., and Doudna, J.A. (2015). Expanding the biologist's toolkit with CRISPR-Cas9. Mol. Cell *58*, 568–574.

Xie, H., Xu, J., Hsu, J.H., Nguyen, M., Fujiwara, Y., Peng, C., and Orkin, S.H. (2014). Polycomb repressive complex 2 regulates normal hematopoietic stem cell function in a developmental-stage-specific manner. Cell Stem Cell *14*, 68–80.